ELSEVIER

Journal of Nuclear Materials 275 (1999) 28–36

journal of nuclear materials

www.elsevier.nl/locate/jnucmat

The mode of stress corrosion cracking in Ni-base alloys in high temperature water containing lead

Seong Sik Hwang *, Hong Pyo Kim, Deok Hyun Lee, Uh Chul Kim, Joung Soo Kim

Steam Generator Materials Project, Korea Atomic Energy Research Institute, P.O. Box 105, Yusong, Taejon 305-600, South Korea

Received 13 March 1998; accepted 31 March 1999

Abstract

The mode of stress corrosion cracking (SCC) in Ni-base alloys in high temperature aqueous solutions containing lead was studied using C-rings and slow strain rate testing (SSRT). The lead concentration, pH and the heat treatment condition of the materials were varied. TEM work was carried out to observe the dislocation behavior in thermally treated (TT) and mill annealed (MA) materials. As a result of the C-ring test in 1M NaOH + 5000 ppm lead solution, intergranular stress corrosion cracking (IGSCC) was found in Alloy 600MA, whereas transgranular stress corrosion cracking (TGSCC) was found in Alloy 600TT and Alloy 690TT. In most solutions used, the SCC resistance increased in the sequence Alloy 600MA, Alloy 600TT and Alloy 690TT. The number of cracks that was observed in Alloy 690TT was less than in Alloy 600TT. However, the maximum crack length in Alloy 690TT was much longer than in Alloy 600TT. As a result of the SSRT, at a nominal strain rate of 1×10^{-7}/s, it was found that 100 ppm lead accelerated the SCC in Alloy 600MA (0.01% C) in pH 10 at 340°C. IGSCC was found in a 100 ppm lead condition, and some TGSCC was detected on the fracture surface of Alloy 600MA cracked in the 10 000 ppm lead solution. The mode of cracking for Alloy 600 and Alloy 690 changed from IGSCC to TGSCC with increasing grain boundary carbide content in the material and lead concentration in the solution. IGSCC seemed to be retarded by stress relaxation around the grain boundaries, and TGSCC in the TT materials seemed to be a result of the crack blunting at grain boundary carbides and the enhanced Ni dissolution with an increase of the lead concentration.

1. Introduction

In spite of the high corrosion resistance of Alloy 600, used as steam generator tubing in pressurized water reactors (PWR), many forms of corrosion take place in the crevices where impurities are accumulated. The mode of cracking in steam generator tubing material is mostly reported to be intergranular in the primary and secondary water environments of PWRs. Recently, however, a mixed mode cracking of steam generator tubing has been found in operating plants around the world, including Korea [1,2]. Lead is believed to be the chemical impurity that induces mixed mode (IG + TG) cracking.

Copson reported first that the stress corrosion cracking (SCC) susceptibility of steam generator tubing could be affected by lead [3]. Several authors have then conducted SCC tests in lead contaminated water and corrosion tests to reveal the role of lead on passive films [4–8].

In this work, SCC tests were performed to examine the role of lead in cracking susceptibility and mode of cracking. Also, TEM work was performed to elucidate the role of grain boundary carbides in transgranular cracking by investigating the dislocation motion in the stressed material.

2. Experimental

The samples used in this work were from commercial Alloy 600 and Alloy 690 steam generator tubing of

* Corresponding author.

0022-3115/99/$ - see front matter
PII: S0022-3115(99)00111-7

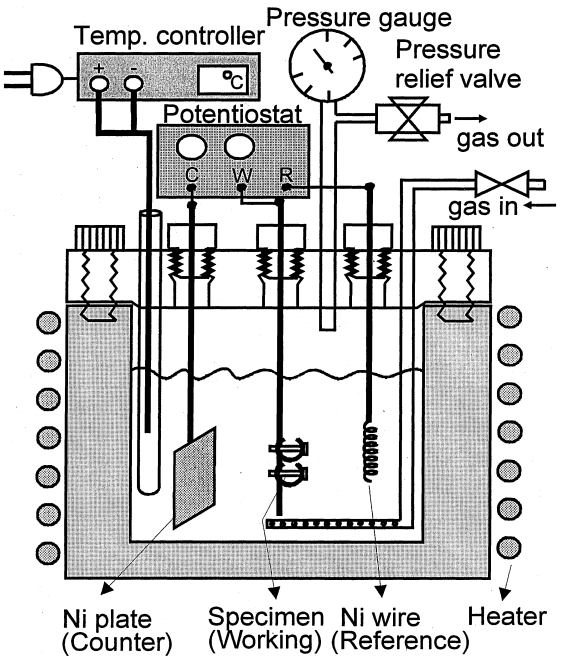

Fig. 1. Schematic of the C-ring test system.

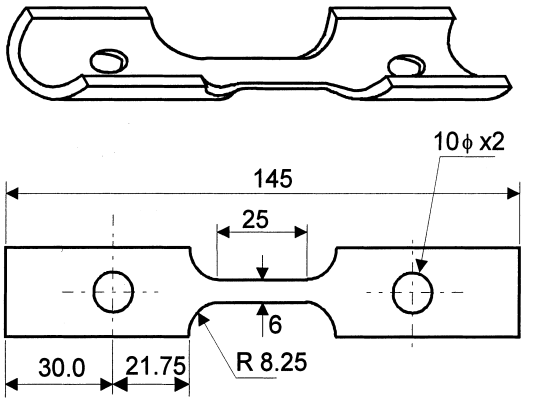

Fig. 2. Dimensions of the SSRT specimen.

22.23 mm outer diameter and 1.27 mm thickness. The chemical composition of the materials is shown in Table 1.

C-ring test specimens were manufactured according to ASTM G38. The apex of the outer surface was ground by #600 emery paper before applying a stress equivalent to 150% of the room temperature yield stress on the C-ring apex. Fig. 1 is a schematic of the SCC test system with C-rings. Alloy 600 bolts and nuts were used to stress the C-rings. A pure nickel wire and plate were used as a reference and counter electrode, respectively. A 1M NaOH test solution was made using distilled and demineralized high purity (18 MΩ cm) water, and PbO was added to the solution to make a concentration of either 100 ppm or 5000 ppm lead. The solution was deaerated using 99.99% nitrogen gas before the tests were performed at 340°C for 20 days. After the immersion test, the specimens were subjected to a metallographic examination by an optical and scanning electron microscope (SEM, ABT DS 130S) equipped with a WDX (Microspec, WDX-3PC).

The slow strain rate testing (SSRT) was conducted in solutions having various lead concentrations and solution pH. Alloy 600MA specimens from the same material as used in the C-ring test, were used in the SSRT. The tubes were split into two pieces longitudinally and machined to give a gauge section 25.4 mm long and 6.0 mm wide. Fig. 2 shows the schematic of the tensile specimen. The gauge section of the specimen was abraded by #600 emery paper. Prior to the test, the specimen was degreased with acetone and cleaned with distilled water. Fig. 3 shows the SSRT test facility, consisting of a Hastelloy C-276 autoclave with a 2 l volume, a pressure balancing pull rod and a control unit. The initial pH of the solution was adjusted by H_2SO_4 or NaOH. Along with this, 100, 5000 and 10 000 ppm lead was added to the solution in the form of PbO. The SSRT was carried out at a temperature of 340°C and at a nominal strain rate of 1×10^{-7}/s.

The dislocation structure of a specimen strained to 0.75% was evaluated using a Philips CM20 TEM. The TEM foil was prepared with jet polishing in a solution of 20% perchloric acid and 80% methanol at −15°C, 150 mA/15VDC. The procedure of the TEM work is presented in Fig. 4.

Table 1
Chemical composition of the materials

Material	Chemical composition (wt%)														
	C	Si	Mn	P	S	Cr	Ni	Co	Mo	Ti	Cu	Al	Fe	B	N
600MA	0.01	0.1	0.3	–	<0.001	15.4	75.1	–	–	0.17	0.2	0.22	8.0	–	–
600TT	0.016	0.32	0.84	0.008	0.003	16.49	72.3	0.016	–	0.32	0.01	0.22	9.36	–	–
690TT	0.02	0.36	0.31	0.010	0.001	30.0	59.6	–	0.013	0.33	0.01	0.023	9.26	0.001	0.033

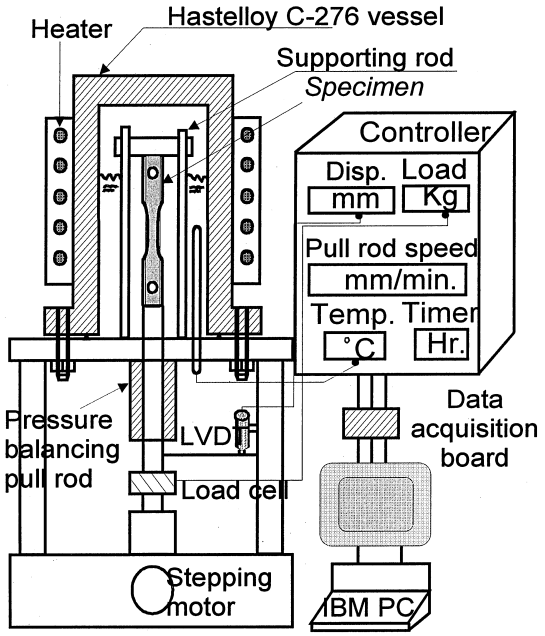

Fig. 3. Schematic of the SSRT machine.

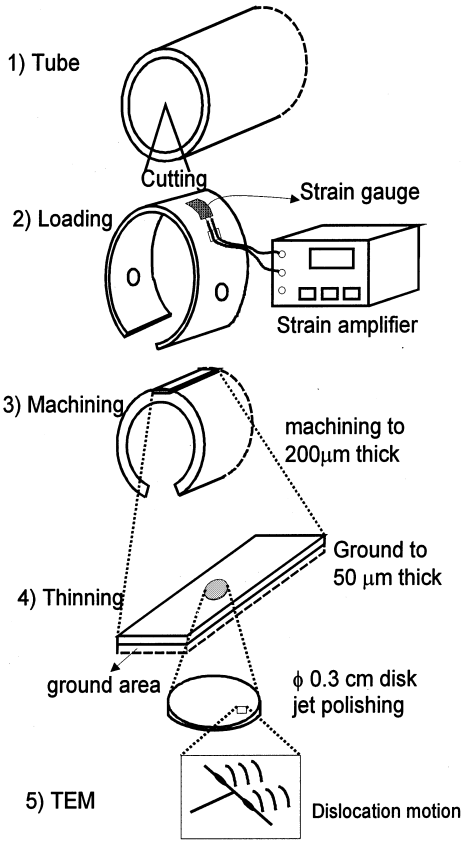

Fig. 4. Procedure of TEM specimen preparation for viewing dislocation motion.

3. Results and discussion

3.1. C-ring test

The mode of intergranular cracking in Alloy 600TT and Alloy 690TT in concentrated caustic solutions has been reported [9,10]. In 1M NaOH solution containing 100 ppm lead and at potentials of +95 and +125 mV vs Ni, Alloy 600MA and Alloy 600TT showed intergranular attack (IGA) and intergranular stress corrosion cracking (IGSCC). The IGA and IGSCC rates increased with the applied potential increasing from 95 to 125 mV vs Ni. Alloy 690TT, however, displayed neither IGA nor IGSCC under these conditions. As the lead concentra-

Table 2
Summary of the C-ring test conditions and results (temperature: 340°C, applied stress: 150% of RTYS, time: 20 days)

Test No.	Solution	Pb at potential, mV vs Ni	Material	Mode of cracking	Average crack propagation rate, μm/h (Maximum)
1	1M NaOH + 100 ppm Pb (Deaerated)	+95	600MA	IGA + IGSCC	0.3 (1.45)
			600TT	IGA + IGSCC	0.15 (0.20)
			690TT	No	–
		+125	600MA	IGA + IGSCC	0.46 (2.1)
			600TT	IGA + IGSCC	0.19 (0.21)
			690TT	No	–
2	1M NaOH + 5000 ppm Pb (Deaerated)	+95	600MA	IGSCC (a little IGA)	0.8 (2.3)
			600TT	TGSCC (no IGA)	0.12 (0.19)
			690TT	TGSCC (no IGA)	0.1 (1.5)

IGA – Intergranular attack, RTYS – Room temperature yield stress, IGSCC – Intergranular stress corrosion cracking and TGSCC – Transgranular stress corrosion cracking.

tion increased from 100 ppm to 5000 ppm in 1M NaOH solution, the mode of cracking in Alloy 600TT changed from IG to TG, while that in Alloy 600MA was still IG, as shown in Fig. 5. An increase of the lead concentration from 100 ppm to 5000 ppm accelerated the IGSCC or transgranular stress corrosion cracking (TGSCC) in Alloy 600MA and Alloy 600TT, but suppressed the IGA in these alloys, as shown in Table 2.

The number of cracks longer than 100 μm within a limited distance (2000 μm) around the C-ring apex was counted. The average crack propagation rate and the maximum crack propagation rate were measured based on a metallographic examination, and were used as a measure of SCC resistance. In the 100 ppm lead solution, in agreement with the the measurement of both the number of cracks and the crack propagation rates, the SCC resistance increased in the sequence Alloy 600MA, Alloy 600TT and Alloy 690TT, as shown in Figs. 6 and 7. The fewest number of cracks was observed for Alloy 690TT, but the maximum crack propagation rate could be much higher than that for Alloy 600TT, as shown in Fig. 8. This result means that Alloy 690TT is not always more resistant than Alloy 600TT. Vaillant et al. have reported a similar test result [6]. In their test in 100 g/l NaOH + 10 g/l PbO solution at 350°C, Alloy 800 exhibited the worst SCC resistance, while Alloy 600TT showed a better resistance compared to Alloy 690TT. The composition of the corrosion product along the crack was analyzed with WDX and is shown in Fig. 9. A significant amount of lead was detected near the crack tip, implying that lead plays a role in the SCC. Fig. 10 shows a SCC ratio (SCC area/total fracture area) of 84% which was observed in Alloy 600MA with 0.01% carbon tested in a solution of pH 10 containing 100 ppm lead at a nominal strain rate of 1×10^{-7}/s at 340°C.

3.2. SSRT

Having been tested in a solution of pH 10, without lead, at 340°C and, at a nominal strain rate of 1×10^{-7}/s,

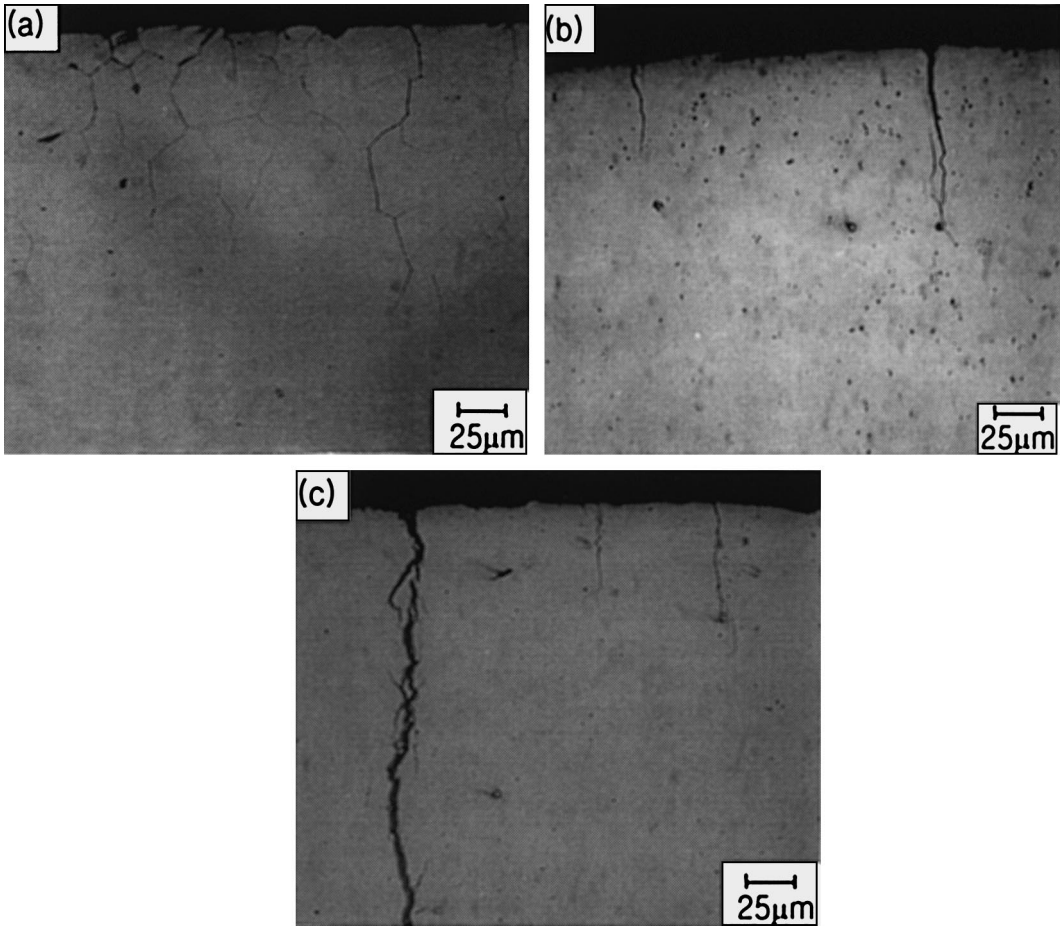

Fig. 5. Different mode of cracking in (a) Alloy 600MA, (b) Alloy 600TT and (c) Alloy 690TT tested in 1M NaOH solution containing 5000 ppm lead at 95 mV vs Ni, for 20 days.

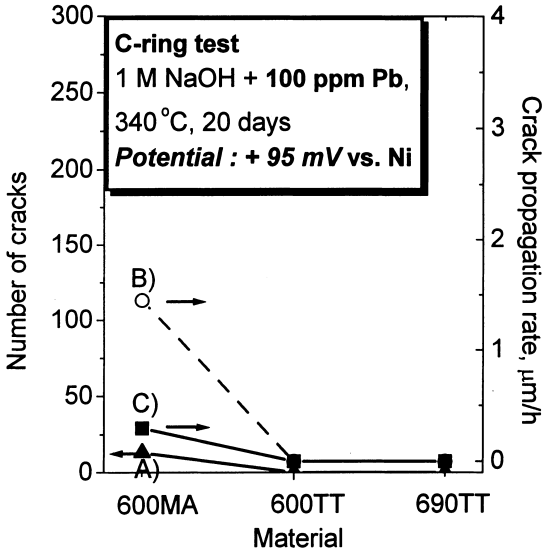

Fig. 6. Comparison of the SCC resistance: (A) the number of cracks (>100 μm) within the limited distance, (B) the maximum crack propagation rate and (C) the average crack propagation rate.

there was no indication of SCC in Alloy 600MA. As shown in Figs. 11 and 12, as the lead concentration increased from 100 ppm to 10 000 ppm, the mode of cracking in the specimen changed from being completely

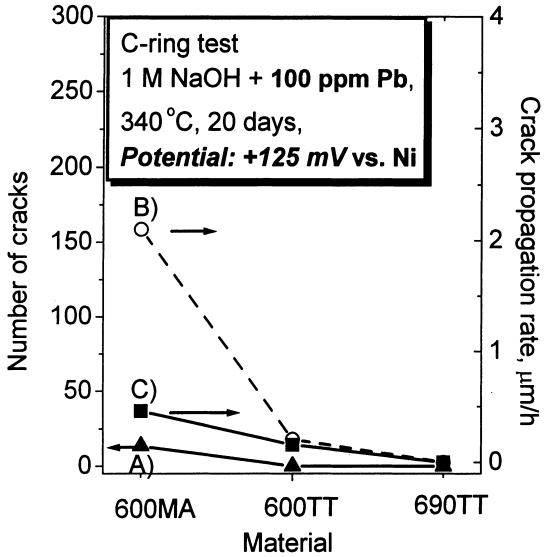

Fig. 7. Comparison of the SCC resistance: (A) the number of cracks (>100 μm) within the limited distance, (B) the maximum crack propagation rate and (C) the average crack propagation rate.

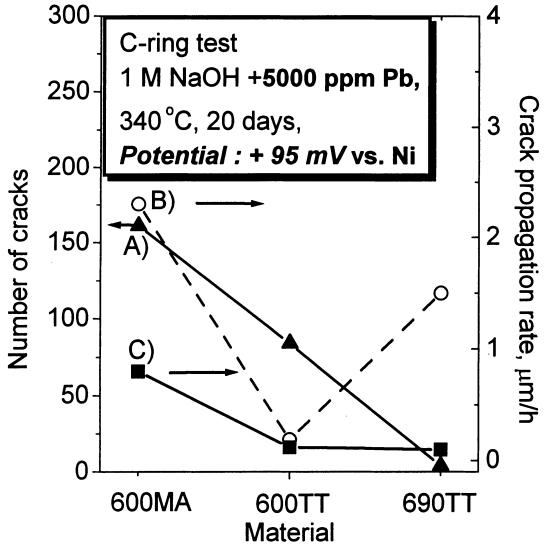

Fig. 8. Comparison of the SCC resistance: (A) the number of cracks (>100 μm) within the limited distance, (B) the maximum crack propagation rate and (C) the average crack propagation rate.

IGSCC to a mixed mode cracking. In 10 000 ppm lead solution, most of the area (99%) was fractured by IGSCC and some TGSCC, as shown in Fig. 12(b). On

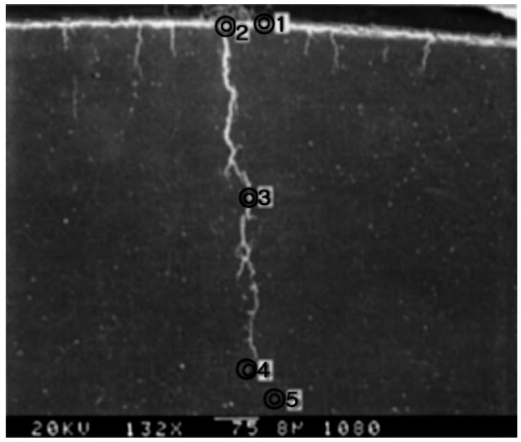

Element(Wt%) Location	O	Pb	Ni	Cr	Fe
1.Near crack	8.92	1.96	49.85	29.79	9.47
2.Crack mouth	4.21	1.39	62.53	24.02	7.85
3.Middle	4.60	1.78	60.69	24.96	7.96
4.Crack tip	4.41	0.12	59.65	27.61	8.21
5.Matrix	0.06	0.00	60.58	30.19	9.17

Fig. 9. Crack morphology and element profile along the crack formed in Alloy 690TT tested in 1M NaOH solution containing 5000 ppm lead at +95 mV vs Ni, for 20 days.

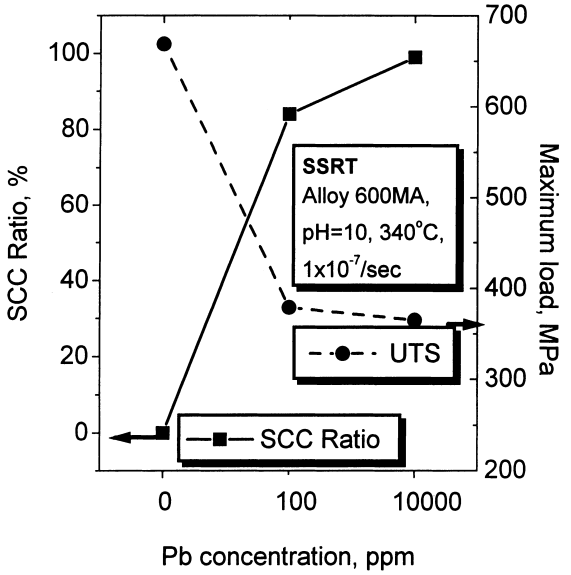

Fig. 10. Effect of the Pb content on the SCC susceptibility of Alloy 600MA in water of pH 10 at 340°C, nominal strain rate 1×10^{-7}/s. SCC ratio: (SCC area/total area) of the fracture surface.

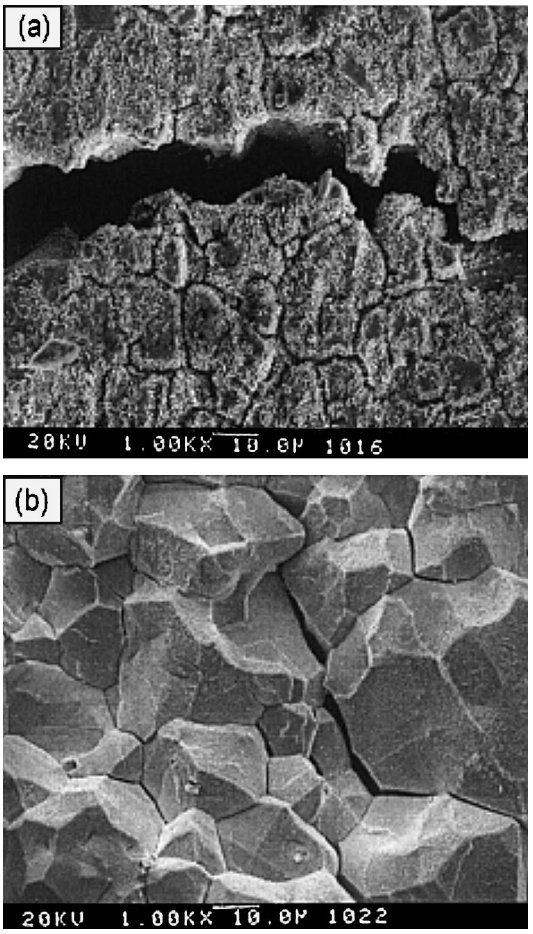

Fig. 11. SEM micrographs of Alloy 600MA (0.01% C) after SSRT in water containing 100 ppm lead at 340°C, pH 10, nominal strain rate 1×10^{-7}/s. (a) Side view of gauge section and (b) fracture surface.

the other hand, as shown in Fig. 11(a), a significant IGA was observed on the Alloy 600MA at 100 ppm lead in a solution of pH 10. Yet, almost no IGA was found in Alloy 600MA which was tested in a solution of pH 10 containing 10,000 ppm lead, as demonstrated in Fig. 12(a). These results are consistent with previous SCC results from the C-ring tests.

PbO, as well as CuO, is considered to be an oxidizer in the secondary side water of steam generators [11], which means that PbO may increase an electrochemical potential of the alloys while reducing to metallic Pb. Table 3 summarizes the SSRT conditions and results for Alloy 600MA.

The pH dependence of the lead cracking was evaluated for Alloy 600MA. SCC did not occur in a pH 7 solution, while 14% of the fracture surface area failed by IGSCC in a pH 4 solution. However, the whole area was fractured by IGSCC in a pH 10 solution. These pH dependences are represented in Figs. 13 and 14. The fracture mode in all pH solutions was intergranular and this lead induced IGSCC is more severer for caustic than for acidic.

3.3. Transmission electron microscopy

To evaluate the difference in cracking modes, the effect of grain boundary carbides on the dislocation behavior in a strained material was examined in TEM. As reported by Bruemmer [12], dislocations in Alloy 600TT seem to be preferentially emitted from grain boundary carbides, and thereby reducing the stress concentration around them, which contributes to an improved IGSCC resistance of Ni base alloys, whereas, a tangled dislocation structure appears in Alloy 600MA near the grain boundary, as shown in Fig. 15.

Lead is reported to enhance the Ni dissolution of Ni-base alloys [13–15]. As shown in Fig. 16(a), a grain boundary crack was retarded at the grain boundary carbide and propagated into the grain. Fig. 16(b) shows a TG crack that propagated into a grain even when it happened to meet a grain boundary. The grain boundaries in TT materials seem to be stress relaxed around the chromium carbide in the grain boundaries. Therefore, another crack path into a grain rather than along a grain boundary can be suggested.

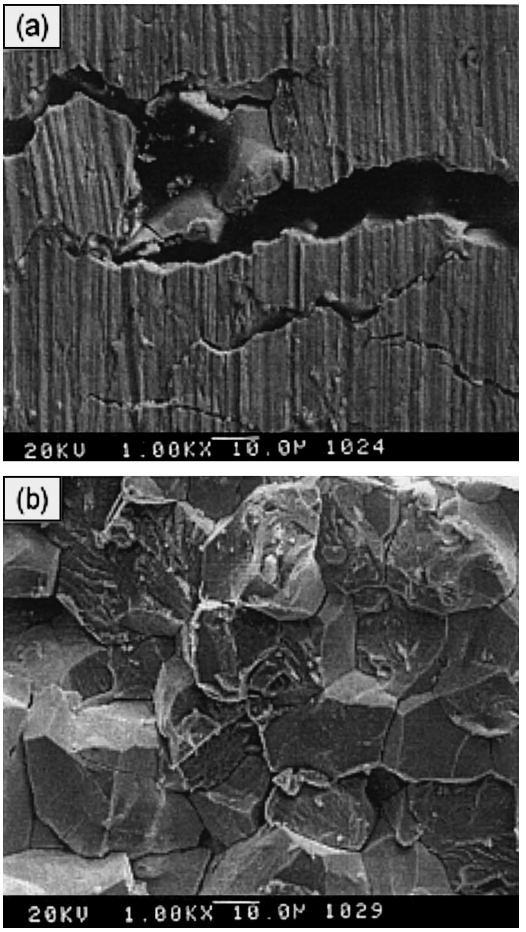

Fig. 12. SEM micrographs of Alloy 600MA (0.01% C) after SSRT in water containing 10 000 ppm lead at 340°C, pH 10, nominal strain rate 1×10^{-7}/s. (a) Side view of gauge section and (b) fracture surface.

The propagation of the transgranular crack can be enhanced by Ni dissolution due to the presence of PbO.

4. Conclusions

1. As lead concentration in the water increases, the mode of SCC in Alloy 600MA changes from being completely IGSCC to a mixed mode with some TGSCC, while that in Alloy 600TT changes from being completely IGSCC to fully TGSCC.
2. IGA of Alloy 600MA and Alloy 600TT is suppressed with an increase of the lead content in the solution.
3. Alloy 690TT is not always more resistant than Alloy 600TT, especially not in caustic solutions with high lead concentrations.

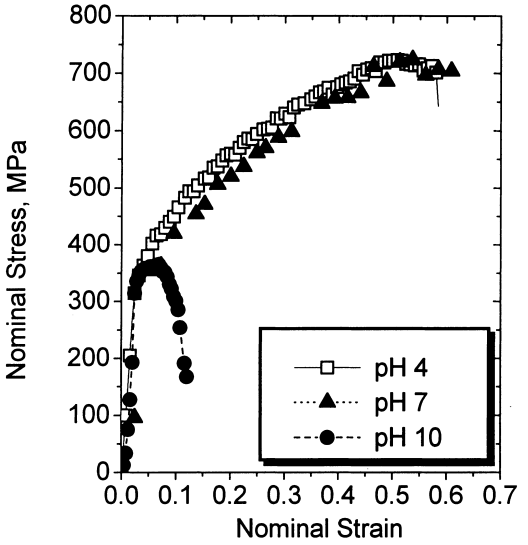

Fig. 13. Stress–strain curves of Alloy 600MA in three different pH conditions at 340°C in water containing 10 000 ppm lead, nominal strain rate 1×10^{-7}/s.

4. IGSCC seems to be retarded by stress relaxation around grain boundary carbides, and TGSCC of TT material is thought to be accelerated by enhanced Ni dissolution due to the presence of lead.

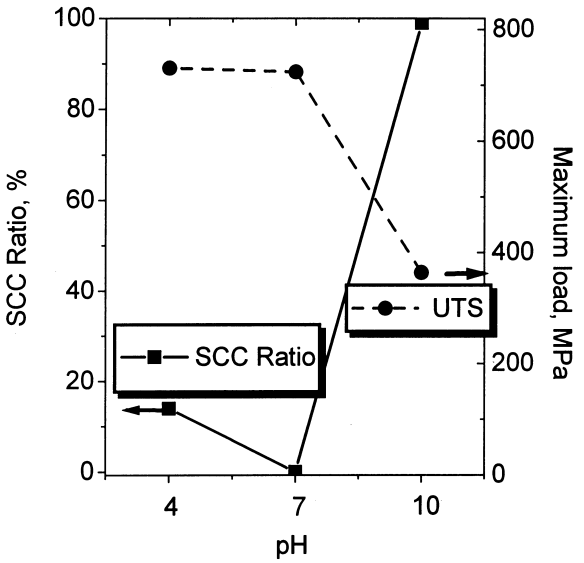

Fig. 14. Effect of pH on the SCC susceptibility of Alloy 600MA in a viewpoint of SCC ratio and maximum load in solution containing 10 000 ppm lead at 340°C, nominal strain rate 1×10^{-7}/s.

Table 3
Summary of the SSRT conditions and results

Test No.	Material	Temperature	Test condition			Result				
			Strain rate (s^{-1})	pH	Pb (ppm)	UTS (MPa)	EL (%)	SCC ratio (%)	Time to failure (h)	Mode of cracking
1	Alloy	340°C	1×10^{-7}	10	0	669	46	0	1368	Ductile
2	600* MA				100	379	12	84	365	IG
3	(0.01% C)				10 000	365	11	99	316	IG(+TG)
4				4	10 000	731	59	14	1631	IG
5				7	10 000	724	62.4	0	1773	Ductile

* Mitsubishi, Heat 906007, MA at 960°C, 10 min.

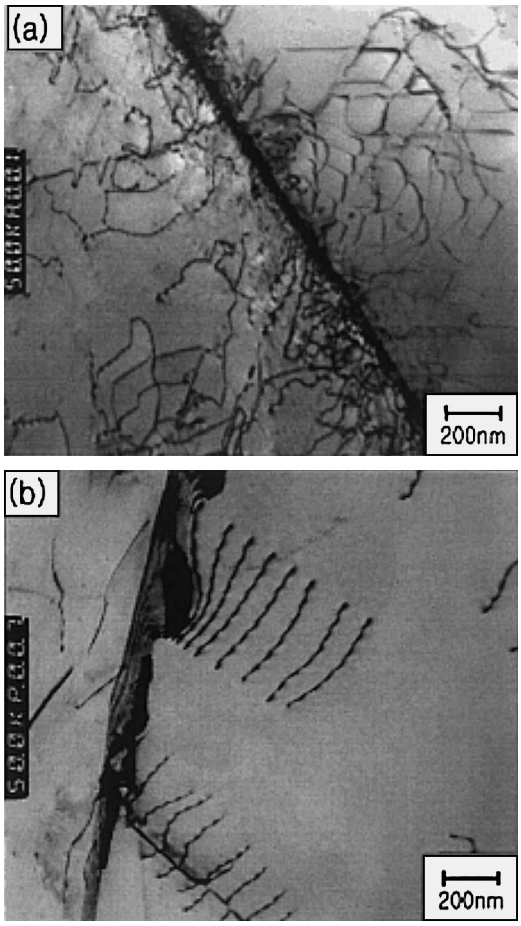

Fig. 15. Comparison of the dislocation motion in (a) Alloy 600 MA deformed 0.75% and (b) Alloy 600TT deformed 0.75%.

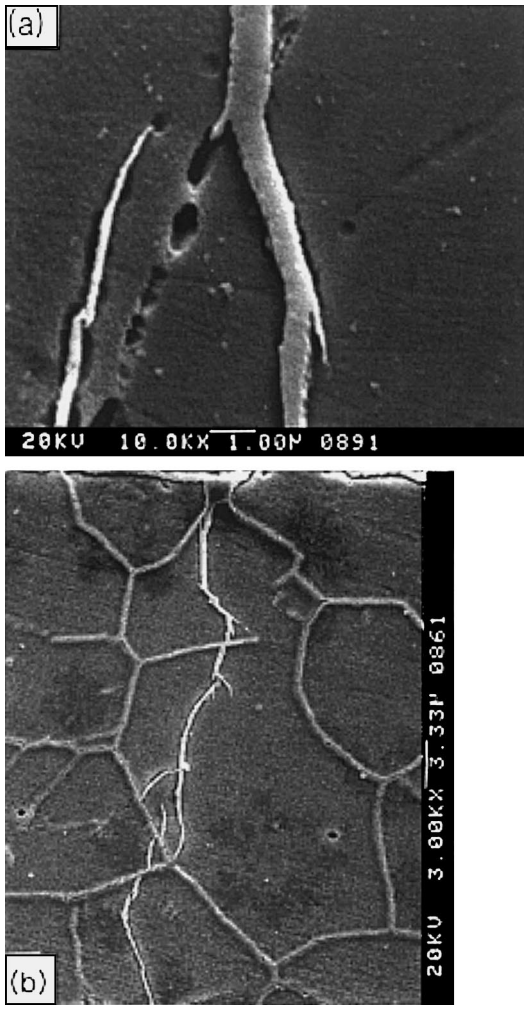

Fig. 16. (a) Grain boundary carbide retards an intergranular crack in a TT alloy and (b) TG crack propagated to different direction in a grain.

References

[1] A.K. Agrawal, J.P.N. Paine, Lead cracking of Alloy 600-A review, in: Proceedings of the Fourth International Symposium on Environmental Degradation of Materials in Nuclear Power Systems–Water Reactors, Jekyll Island, Georgia, USA, 6–10 August, 1989, p. 71.

[2] S.S. Hwang, J.S. Kim, U.C. Kim, Failure analysis report of the steam generator tubings pulled out from Kori unit 2, Korea Atomic Energy Research Institute, 1990.

[3] H.R. Copson, S.W. Dean, Corrosion 21 (1965) 1.

[4] T. Sakai, S. Okabayashi, K. Aoki, K. Matsumoto, Y. Kishi, A study of oxide thin film of Alloy 600 in high temperature water containing lead, CORROSION/90, paper no. 520.
[5] M. Helie, Lead assisted stress corrosion cracking of Alloys 600, 690 and 800, in: Proceedings of the Sixth International Symposium on Environmental Degradation of Materials in Nuclear Power Systems–Water Reactors, Sandiego, California, USA, 1–5 August, 1993, p. 179.
[6] F. Vaillant, Comparative behavior of Alloys 600, 690 and 800, in: Proceedings of the Seventh International Symposium Environmental Degradation of Materials in Nuclear Power Systems – Water Reactors, Breckenridge, Colorado, USA, 7–10 August, 1995, p. 219.
[7] B.P. Miglin, J.M. Sarver, M.J. Psaila-Dombrowski, P.E. Doherty, Lead assisted stress corrosion cracking of nuclear steam generator tubing materials, Proceedings of a conference jointly sponsored by the EPRI and ANL, Airlie, Virginia, USA, 9–13 October, 1995, p. 305.
[8] S.S. Hwang, U.C. Kim, Y.S. Park, J. Nucl. Mater. 246 (1997) 77.
[9] R.J. Jacko, Corrosion evaluation of thermally treated Alloy 600 tubing in primary and faulted secondary water environments, EPRI NP-6721-SD, June 1990, pp. 3–103.
[10] R.J. Jacko, Stress corrosion testing of candidate steam generator tubing materials, in: Proceedings of Workshop on Thermally Treated Alloy 690 Tubes for Nuclear Steam Generators, EPRI NP-4665S-SR, July 1986, pp. 1–15.
[11] J.P.N. Paine, R.S. Pathania, C.E. Shoemaker, Effect of caustic environment on intergranular attack and stress corrosion cracking of Alloy 600, in: Proceedings of the Third International Symposium on Environmental Degradation of Materials in Nuclear Power Systems – Water Reactors, Traverse City, Michigan, USA, 30 August–3 Septemper, 1987, p. 501.
[12] S.M. Bruemmer, Corrosion 44 (1988) 782.
[13] S.S. Hwang, U.C. Kim, Y.S. Park, J. Corros. Science Society of Korea 25 (1996) 170.
[14] T. Sakai, T. Senjuh, K. Aoki, T. Shigemitsu, Y. Kishi, Lead induced stress corrosion cracking of Alloy 600 and 690 in high temperature water, in: Proceedings of the Fifth International Symposium on Environmental Degradation of Materials in Nuclear Power System – Water Reactors, Monterey, California, USA, 25–29 August, 1991, p. 764.
[15] M.D. Wright, G. Goszczynski, F. Peca, Embrittlement of Alloy 400 by lead in secondary side steam generator environments, in: Proceedings of the Seventh International Symposium on Environmental Degradation of Materials in Nuclear Power Systems –Water Reactors, Breckenridge, Colorado, USA, 7–10 August, 1995, p. 209.